CSCE Annual Conference
Growing with youth – Croître avec les jeunes

Laval (Greater Montreal)
June 12 - 15, 2019

ASSESSMENT OF REPAIR TECHNIQUES FOR GFRP REINFORCED BRIDGE BARRIERS USING VECTOR2

Aljaaidi, A.[1,2] and Tomlinson, D[1,3].
[1] University of Alberta, Canada
[2] aljaaidi@ualberta.ca
[3] dtomlins@ualberta.ca

Abstract: A parametric study using a finite element analysis software (VecTor2) was conducted to investigate the efficiency of proposed repair techniques for bridge barriers reinforced with glass fibre-reinforced polymer (GFRP) bars. Before that, since Alberta transportation test level four (TL-4) bridge barriers design has never been experimentally tested with GFRP bars as reinforcement instead of steel, and to justify this replacement, three models of bridge barriers mimicking the design and detailing of Alberta Transportation TL-4 bridge barriers and representative of the as built conditions were put together and tested in VecTor2. These models were subjected to a displacement rate analysis until failure to evaluate their ultimate load-carrying capacities. After one of the models reinforced with GFRP reinforcement proved a comparable strength to its counterpart reinforced with steel, it was used as a reference model to evaluate the behavior of the models representing the repair techniques. In the proposed repair techniques, the new barrier wall is anchored to the existing bridge deck using single headed GFRP bars. This paper investigated the efficiency of the repair techniques in terms of ultimate load-carrying capacity and deflection, as well as the effect of different embedment lengths, and the different spacings of single-headed GFRP bars and different diameters on the ultimate load carrying capacity The data generated from this parametric study were compared and discussed, and some recommendations and conclusions were drawn. The next stage of this project will be to experimentally test and validate those models to verify the validity of using GFRP reinforcement in Alberta TL-4 bridge barriers instead of steel, and the efficacy of the proposed repair techniques.

1 INTRODUCTION

Fibre reinforced polymer reinforcement, especially Glass Fibre Reinforced Polymers (GFRP), has emerged as an alternative to traditional steel reinforcement in concrete structures. GFRP reinforcement is particularly useful in infrastructure applications due to its superior corrosion resistance relative to steel (Ahmed et al. 2011). Moreover, it is a feasible and practical replacement for steel in bridge construction, particularly in bridge decks and barriers, based on its structural performance and cost-effectiveness (El-Salakawy and Islam 2014). The use of GFRP bars in reinforced concrete bridge deck slabs and barriers has significantly increased in Canada (Ahmed et al. 2013).

Based on the performance/test level, there are six different types of barrier walls, namely Test Level 1 (TL-1) to Test Level 6 (TL-6). The design and selection of a bridge barrier is based upon an exposure index that depends on traffic conditions, surrounding environment, the expected frequency and consequences of vehicle accidents, and bridge site. The required minimum test level is selected based on two major factors: the minimum height and the structural adequacy (impact capacity) of the bridge barrier. Among those types, TL-4 is the most used type in Alberta and was investigated in this study. In static testing of a TL-4 traffic barriers, CSA S6-14 requires that the barrier wall should be able to resist a transverse load of 100 KN applied over a barrier length of 1050 mm at a height of 700 mm above the deck. Moreover, the minimum

height of the barrier wall should be 800 mm (CSA S6-14). Nevertheless, both Canadian Standards Association (CSA) S6-14 (the Canadian Highway Bridge Design Code (CHBDC)) and American Association of State Highway and Transportation Officials (AASHTO) design specifications (2007) specify that bridge barriers should be crash-tested to evaluate their overall performance. However, both codes allow using specified static monotonic loads equivalent to vehicle impact to start the design of reinforcement and anchorage of bridge barrier wall-deck overhang (CSA S6-14) (AASHTO 2007).

Although CSA S6-14 provides guidelines on designing concrete bridge barriers reinforced with GFRP bars, it does not provide guidelines on repairing or rehabilitating concrete bridge barriers reinforced with GFRP bars in case of damage caused by factors such as: exposure to freeze-thaw or wet-dry cycles, poor quality construction, poor design details, inadequate maintenance, changes in level of service, and vehicle collision. Bridge barriers, due to their primary function to reduce the consequences of vehicles leaving the roadway, are susceptible to local damage and excessive cracking caused by vehicle impact. This poses concerns regarding the feasibility and economics of repairing concrete bridge elements reinforced with FRP materials. El-Salakawy et al. (2010) investigated the feasibility and effectiveness of repairing GFRP reinforced slabs and addressed two major questions: (1) what is the most suitable concrete demolition technique that causes minimal damage to the GFRP bars, and (2) how effective is this technique in terms of the flexural strength and load-transfer efficiency of concrete slabs. It was concluded that traditional concrete demolition techniques such as jackhammering and hydro-demolition resulted in severe damage to the existing GFRP reinforcement which rendered it inadequate to resist tension. Therefore, It was recommended that the damaged concrete be saw-cut for the full-depth removal of concrete, and the interrupted reinforcement should be replaced with new FRP bars using either the planting (splicing) or the Near-Surface Mounting (NSM) technique.

As a result, El-Salakawy et al. (2014) tested two repair techniques for bridge barriers on double slope performance level (PL-2) barriers, namely the planting and the NSM techniques. Both techniques showed satisfactory structural performance. Nevertheless, executing them in practice for long bridge segments requires considerable time and effort due to the drilling involved at tight spacings to splice the original bars to new ones, or saw-cutting grooves on the concrete surface to install NSM bars. Therefore, the overall objective of this project is to investigate the efficiency, practicality, and cost-effectiveness of two new repair techniques for bridge barriers reinforced with GFRP.

Both techniques involve saw-cutting to remove damaged barrier walls, and then drilling holes into the overhang deck slabs to plant single-headed GFRP bars which transfer impact loads from the barrier wall to the overhanging deck slab. GFRP bent bars have been used in the past to provide sufficient anchorage at the barrier wall-deck interface. However, because of the direction and rearrangement of the fibres in the bend the tensile capacity is significantly reduced. For instance, the ultimate tensile strength of GFRP bars with 50 GPa modulus of elasticity decreases from 1000 MPa to 450 MPa (45% reduction) at the bent portion compared with the straight portion of the bars (TUF-BAR Canada 2019). Azimi et al. (2014) studied the anchorage sufficiency of the proposed barrier wall-deck slab connection reinforced with single-headed GFRP bars and concluded that these bars can be used in bridge barrier walls to resist the applied vehicle impact load specified in the CSA S6-14 at the barrier wall-to-deck slab junction. Nevertheless, they used a different orientation of the single-headed GFRP bars than the one proposed in this project with the head of the GFRP bars embedded in the deck slab. It is worth mentioning that they tested Performance level 2 and 3 (PL-2 and PL-3) types of barriers with single and double slopes barrier walls.

2 METHODOLOGY

This research comprises two major stages. The first stage, described in this paper, involves the assessment of the as built design and the repair techniques for GFRP reinforced bridge barriers using the finite element program VecTor2. The second stage will be the testing and verification of the results of stage one in the lab.

Stage one is divided into two phases. The first phase includes the assessment of the as-built bridge barriers using VecTor2. In this phase, test level 4 (TL-4) single slope bridge barrier prototypes conforming to the detailing scheme (same layout and spacing of bars) of a successfully crash-tested steel reinforced concrete

bridge barriers commonly used in Alberta (Figure 1(a)) are modeled with steel and GFRP as reinforcement in FormWorks (a pre-processor software for VecTor2) (Figure 1(b)). One model is reinforced with steel, to be used as a control model, while the others are reinforced GFRP reinforcement, which are yet to be crash-tested. These models are then analyzed by utilizing a displacement controlled loading at a height of 690 mm above the deck slab, which represent an equivalent static load to simulate the impact load, using VecTor2 software. The results are then analyzed using Augustus (a post-processor for VecTor2).

The second phase is the assessment of the repair techniques for GFRP reinforced bridge barriers using VecTor2. In this phase, single-headed GFRP bars are used as connections between the deck slab and the barrier wall to transfer the loads. The layers of GFRP bars in the barrier wall are terminated at the interface of barrier wall and the deck slab to reflect the saw-cutting of the previous GFRP bars. The spacing, diameter, and embedment depths of the anchorage systems are the main parameters investigated in the repair technique.

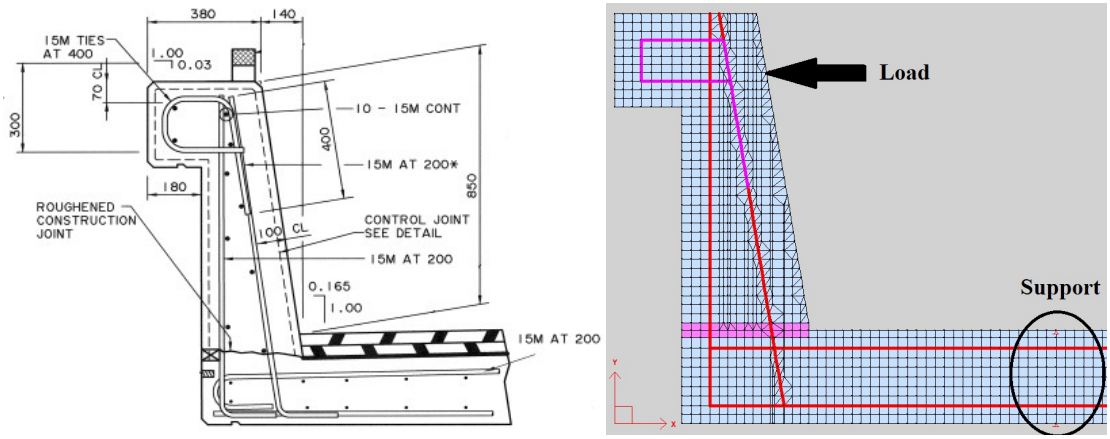

Figure 1: Bridge Barriers: (a) Alberta TL-4 design (Alberta Transportation 2017). (b) Alberta TL-4 (VecTor2 Model).

2.1 Repair Techniques

Two techniques will be utilized to repair the damaged bridge barriers. Both techniques involve saw-cutting to remove the damaged barriers, and then drilling holes into the overhang deck slabs to plant single-headed GFRP bars which transfer impact loads from the barrier wall to the overhang deck slab. Epoxy is injected in the drilled holes before the placement of GFRP bars to hold them in place and transfer loads. The difference between these techniques is that in one repair technique a single-assembly of GFRP bars is used on the traffic side of the barrier wall to reinforce Fibre-Reinforced Concrete (FRC) (Figure 2(a)). In the other technique, a double-assembly of GFRP bars will be utilized to reinforce plain concrete (Figure 2(b)).

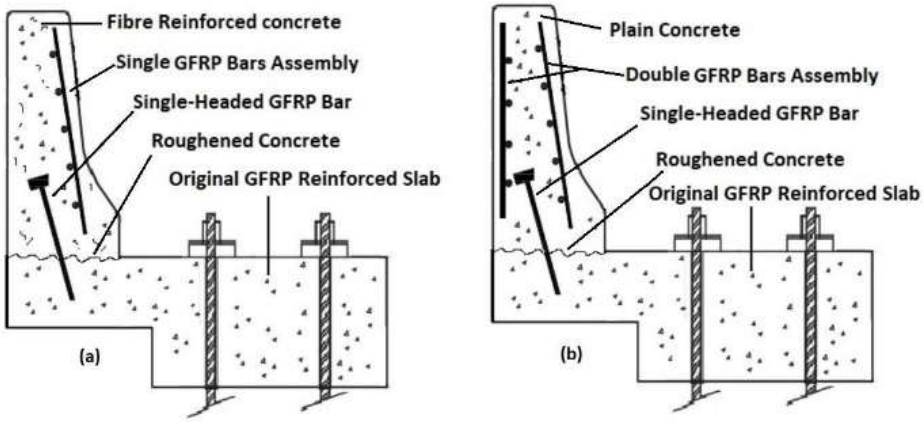

Figure2: Repair techniques (a) FRC with single assembly, (b) Plain concrete with double assembly.

2.2 Model Description

2.2.1 VecTor2 Overview

VecTor2 is a non-linear finite element program developed at the University of Toronto for the analysis of two-dimensional reinforced concrete membrane structures. It provides assessment of the structural performance of reinforced concrete in terms of strength, post-peak behaviour, failure mode, deflections, and cracking by combining non-linear constitutive models for reinforced concrete and reinforcement.

VecTor2 uses the Modified Compression Field Theory and the Disturbed Stress Field Model to predict the response of reinforced concrete elements. It utilizes an incremental total load, iterative secant stiffness algorithm to complete nonlinear analysis (Wong et al. 2013).

The FormWorks preprocessor software helps in using VecTor2 as an analytical tool, by decreasing the potential for input error and expediting the modeling process through a graphical interface for data input and visualization in the Windows environment. After the analysis is done using VecTor2, Augustus software provides graphical post-processing capabilities for the analysis results.

2.2.2 Bridge Barrier Model Details and Material Properties

The barriers and overhangs were modeled using 2-D plane membrane elements. The maximum mesh sizes were taken as 25x25 mm, with an aspect ratio of 1.5. View of the FEA model is shown in Figure 1. The thickness of the elements was 1000 mm which represents the width of the barrier overhang (i.e. results are provided for a metre unit width of barrier/deck). The models are defined using three regions of concrete: One region represents the deck slab, another represents the barrier wall, and the third one represents the interface between the deck slab and the barrier wall. The support condition was taken as four pin supports in pairs at 1000 mm apart, one pair of them at 500 mm from the end of the deck. This support condition is representative of the support condition expected in the lab. This support condition also represents the expected support conditions provided by girders in actual bridges.

Three models were built with different reinforcement to represent as-built conditions. All models had concrete cover of 40 mm for the slab, 100 mm for the front face of the barrier wall, and 75 mm for the back face of the barrier wall. In addition, they had a bar spacing of 200 mm. One model was totally reinforced with 15M steel bars (area per bar is 200 mm^2), the second one was reinforced with 15M GFRP bars, the third one was reinforced with 20M GFRP bars (area per bar is 300 mm^2).

The concrete was modelled using Hognestad model for pre-peak compression, Modified Park-Kent model for post-peak compression, Vecchio 1992-A model for compression softening, Modified Bentz 2003 model for tension stiffening, and linear tension softening model. The concrete compressive strength is 35 MPa and tensile strength is 1.95 MPa. The concrete is normal density (2400 kg/m^3) with a maximum aggregate size of 10 mm.

For the barrier walls repaired with fibre-reinforced concrete FRC, hooked steel fibres with 1050 MPa tensile strength are used. Their length and diameter are 60 mm and 0.75 mm, respectively. And the fibre volume fraction used is 1%. The Simplified Diverse Embedment Model (SDEM) for monotonic loading conditions is used to consider the contribution of steel fibre reinforcement to concrete tensile strength.

The steel reinforcement was modelled with a 400 MPa yield strength, 600 MPa ultimate strength, and a 200 GPa modulus of elasticity. The ultimate tensile strain is 10% and the strain hardening strain is 1.2%.

The GFRP bars was modelled as linear-elastic until failure with a 1200 MPa ultimate strength, 60 GPa modulus of elasticity, and 10% ultimate tensile strain. These GFRP properties are representative of high modulus GFRP bars available from manufacturers. GFRP single-headed bars have the same material properties as straight bars.

2.2.3 Analysis

All model were loaded, as described earlier, under an increasing monotonic displacement until a specified displacement of 60 mm was reached. Each model consisted of 61 (displacement) stages. The first stage started with zero displacement which represented the origin point (0, 0), and then the displacement proportionally increased by a common factor of 1 mm from one load stage to the next. A load step of 1 mm displacement was chosen to allow the solution to properly converge in a fewer number of iterations before the analysis proceeds to the next load step since the improper convergence may overestimate the strength for the imposed displacement which might misrepresent the overall softening response of concrete. To control the quality of the analysis and to ensure that it resembles the experimental testing in the lab, a Static Nonlinear-Load Step analysis was chosen, a maximum number of 60 iterations of was set, and a convergence limit of 1.00001 was applied in the Analysis Parameters Group.

2.3 General Considerations

CSA S6-14 and the AASHTO Load and Resistance Factor Design (LRFD) codes do not provide specific guidance for acceptable horizontal deflection of the barrier wall caused by vehicle impact. Hence, the ultimate load carrying capacity was used as the main parameter to evaluate the performance of the barrier overhang and the different repair techniques. However, new designs of bridge barriers should be crash tested. In the case of dynamic testing, greater horizontal deflection of the barrier wall may play a favourable role in absorbing energy of vehicle impact caused by the nonlinearity of concrete (Azimi et al. 2014).

3 Results and Discussion

3.1 Comparison between Steel- and GFRP-reinforced as-built bridge barriers

The model of the bridge barrier reinforced with steel exhibited a ductile behaviour with high deflection at the maximum load (Figure 3). The ultimate load capacity was 100 kN (all capacities are per metre length of barrier) with a horizontal deflection of 40 mm at the point of load application. On the other hand, the models reinforced with GFRP bars (15M and 20M) showed lower deflections at lower loads. For instance, when 15M bars were used the ultimate load carrying capacity was 79.3 kN with a horizontal deflection of 29.8 mm at the point of load application. In the case of using 20M bars, the ultimate load carrying capacity was 92.1 kN with a horizontal deflection of 24.8 mm. The design of bridge barriers is an extreme event limit state, therefore, using 20M GFRP bars in TL-4 bridge barriers could be a viable option since its model achieved 101% of the ultimate load carrying capacity (at yield) of its counterpart model reinforced with steel.

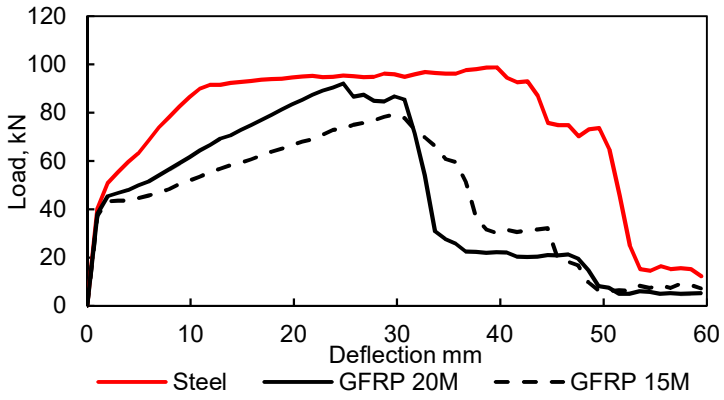

Figure 3: Comparison between Steel and GFRP reinforced models.

3.2 Comparison between the proposed repair techniques

The models of the repair techniques on GFRP bridge barriers reinforced with 15M bars at a spacing of 200 mm are compared against the as-built model. The model of the repaired barrier using FRC with single

assembly of GFRP bars and single-headed GFRP bars resisted a maximum load of 75.9 kN at a horizontal displacement of 26.8 mm when the GFRP single-headed bars were spaced at 200 mm and 81% embedded in the deck slab. On the other hand, the model of the repaired barrier using plain concrete with double assembly of GFRP bars resisted a maximum load of 74.4 kN at a horizontal displacement of 28.2 mm when the GFRP single-headed bars were spaced at 200 mm and 81% embedded in the deck slab. Both repair techniques models had load carrying capacity lower than the model of the as built barrier which resisted a maximum load of 79.3 kN at a horizontal displacement of 29.8 mm (Figure 4). However, the difference is fairly small (roughly 5%). The repair technique using FRC achieved a slightly higher capacity due to the presence of steel fibres which help in resisting the tensile stresses in concrete. It is worth mentioning that repairing barriers using FRC with single assembly of GFRP bars requires less time and effort compared to using RC with double assembly of GFRP bars. Table 1 shows sample results of the repaired models, using both techniques with GFRP single-headed bars (15M and 20M) spaced at 200 mm and embedment ratio of 81% for both GFRP reinforcement schemes (15M and 20M).

Table 1: Ultimate load carrying capacity and deflection at max. load of repaired models.

Model	Strength, kN	% of As-built model	Deflection @ max load, mm
GFRP 20M (As-built)	92.1	100 (reference)	24.8
GFRP 20M FRC repaired	93.7	101.8	27.8
GFRP 20M RC repaired	88.8	96.4	23
GFRP 15M (As-built)	79.3	100 (reference)	29.8
GFRP 15M FRC repaired	75.9	95.7	26.8
GFRP 15M RC repaired	74.4	93.8	28.2

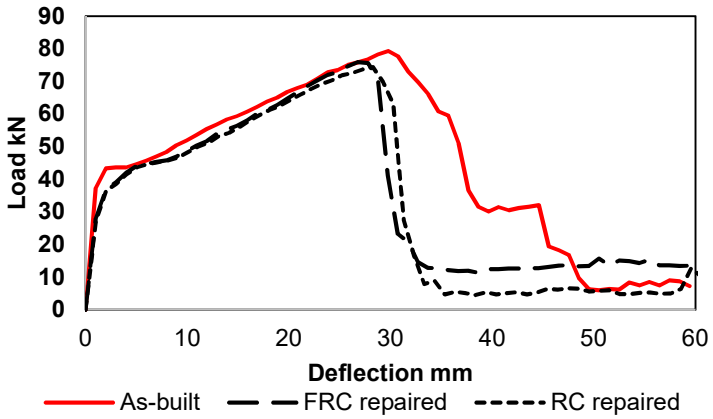

Figure 4: Comparison between the proposed repair techniques models.

3.3 Parametric study on one of the repair techniques using VecTor2:

This parametric study was carried out to investigate the effect of parameters on the effectiveness of one of the proposed repair techniques on the overall performance of the repaired barriers. The technique focused on plain concrete reinforced with 15M and 20M GFRP bars spaced at 200 mm repaired with a double assembly of 15M GFRP bars spaced at 200 mm. The undamaged 20M GFRP bridge barrier model was used as a reference for evaluating the performance of the repaired GFRP bridge barriers models after it had proven a satisfactory behaviour compared to its steel-reinforced counterpart. The spacing, s, diameter, d_b, and embedment depth percentage, $E\%$, of the anchorage systems were the main parameters investigated. The associated values for each parameter were taken as: s (100, 150, and 200 mm), d_b (15 mm, and 20 mm), and E% (50, 81 (embedded to the level of bottom reinforcement of the deck slab), and 100(full depth embedment) %). The FEA models were built to represent single-sloped TL-4 Alberta

Transportation bridge barriers, which represent one of the most common types of barriers used in Alberta. Thirty 2-D finite element models were constructed with different parameters and then subjected to a monotonic displacement loading at a height of 690 mm above the deck level (250mm) as shown in Figure 1(b).

Representative results obtained from FEA are shown in Figures 5 and 6, illustrating the effect the spacing, diameter, and embedment depth percentage of the GFRP single-headed bars on the ultimate load capacity P. The results of all of the models are shown in Table 2, including the corresponding horizontal displacement at the loading point (940mm) at peak load. In Table 2, the Models are identified based on the following process: reinforcement material, main reinforcement diameter (single-headed GFRP bar diameter — headed bar embedment ratio - headed bar spacing). The as-built GFRP model reinforced with 20M bars as main reinforcement is used as a reference since it exhibited a comparable load carrying capacity to its steel-reinforced counterpart (at yield).

Table 2: Ultimate load carrying capacity and deflection at max. load of the models.

Model ID	Strength (kN)	% of reference model	Deflection @ max load (mm)
GFRP 20M (As-built) (Reference)	92.1	100	24.8
GFRP 15M (As-built)	79.3	86	29.8
Steel 15M (As-built)	91.6 (Yield)	99.5	12.9
GFRP 20M (20M - 100% - 100 mm)	126.9	138	38.7
GFRP 20M (20M - 100% - 150 mm)	118.9	129	40.6
GFRP 20M (20M - 100% - 200 mm)	111	121	36.7
GFRP 20M (20M - 81% - 100 mm)	94.5	103	27
GFRP 20M (20M - 81% - 150 mm)	90.3	98.0	27
GFRP 20M (20M - 81% - 200 mm)	88.8	96.4	23
GFRP 20M (20M - 50% - 100 mm)	71.5	77.6	16.7
GFRP 20M (20M - 50% - 150 mm)	70.6	76.7	18.7
GFRP 20M (20M - 50% - 200 mm)	70.4	76.4	18.7
GFRP 15M (20M - 100% - 100 mm)	105.2	114	42.6
GFRP 15M (20M - 100% - 150 mm)	94.6	102.7	40.6
GFRP 15M (20M - 100% - 200 mm)	92.9	101	40.6
GFRP 15M (20M - 81% - 100 mm)	83	90	29
GFRP 15M (20M - 81% - 150 mm)	78.3	85	27
GFRP 15M (20M - 81% - 200 mm)	73.6	80	25.2
GFRP 15M (20M - 50% - 100 mm)	63.6	69	18.7
GFRP 15M (20M - 50% - 150 mm)	61.4	66.7	20.6
GFRP 15M (20M - 50% - 200 mm)	58.9	64	18.7
GFRP 15M (15M - 100% - 100 mm)	101	109.7	43.6
GFRP 15M (15M - 100% - 150 mm)	92.7	100.7	40.6
GFRP 15M (15M - 100% - 200 mm)	85.6	93	37.7
GFRP 15M (15M - 81% - 100 mm)	80.2	87	28.2
GFRP 15M (15M - 81% - 150 mm)	76.3	83	27.2
GFRP 15M (15M - 81% - 200 mm)	74.4	80.8	28.2
GFRP 15M (15M - 50% - 100 mm)	63.0	68.4	18.7
GFRP 15M (15M - 50% - 150 mm)	59.4	64.5	19.7
GFRP 15M (15M - 50% - 200 mm)	59.4	64.5	19.7

3.3.1 Effect of headed bar spacing

For all the embedment ratios using single-headed 15M GFRP bars, the ultimate load carrying capacity P is affected by the spacing S. For instance, for the barrier with 15M single-headed bars and 81% embedment ratio, P is increased by 7.8% from 74.4 KN to 80.2 KN when the spacing is decreased from 200 mm to 100

mm. However, the ultimate capacity was not affected by the change in spacing from 200 mm to 150 mm when the embedment ratio was 50%. Nevertheless, the ultimate capacity was increased when the spacing was decreased from 150 mm to 100 mm.

3.3.2 Effect of headed bar diameter

In the case of different diameters of single-headed GFRP anchorage while fixing the spacing, the ultimate load carrying capacities observed were comparable for different diameters at lower embedment ratios, however, the model repaired with the larger diameter (20M) showed higher capacity at higher embedment ratios. Again, this was caused by the mode of failure involved. Since the larger diameter needs a longer depth of embedment to develop its capacity, it showed higher capacity at the higher end of embedment ratio compared to the smaller diameter.

3.3.3 Effect of headed bar embedment depth

For the same diameter of single-headed GFRP anchorage and the same spacing, the ultimate load carrying capacity increased with the increased embedment ratio due to the pull-out mode of failure. Moreover, the displacement associated with the maximum load also increased with the increased embedment ratio for the same reason. Unlike the consistent relationship between the spacing and the ultimate load carrying capacity across different embedment ratios, there was no common trend in the change in the displacement at the maximum load capacity at different spacings across different embedment ratios.

3.3.4 Comparison between repaired and as-built models

In comparison with the as-built capacity, the barrier models repaired with 15M bars planted at full depth (100%) achieved higher capacities than the model of the as built barrier (Figures 5 and 6). On the other hand, the models in which the embedment ratio was 50% achieved lower capacities, for example, the reduction in strength was 20.6% at a spacing of 100mm (figure 5(a)). However, when the same spacing was used with an 81% embedment ratio, the capacity was slightly higher than the as-built model.

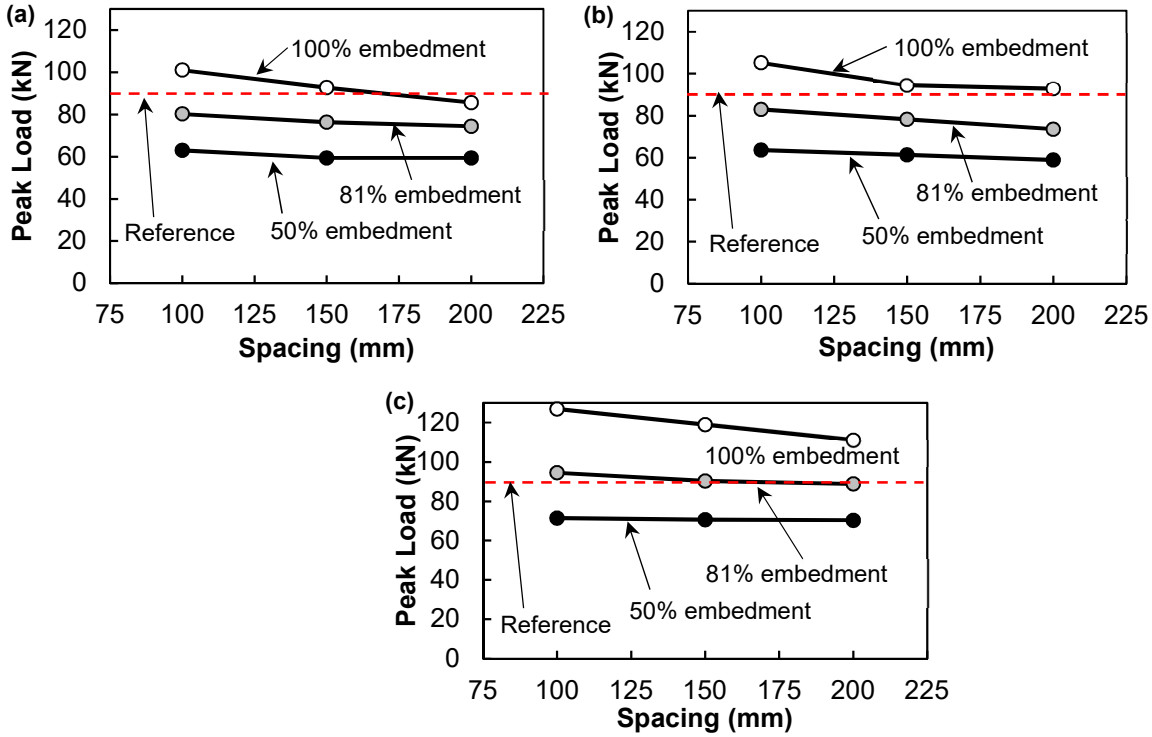

Figure 5: Effect of bar spacing on barrier peak load for (a) 15 mm GFRP retrofit on 15M reinforced barrier (b) 20 mm GFRP retrofit on 15M reinforced barrier (c) 20 mm GFRP retrofit on 20M reinforced barrier.

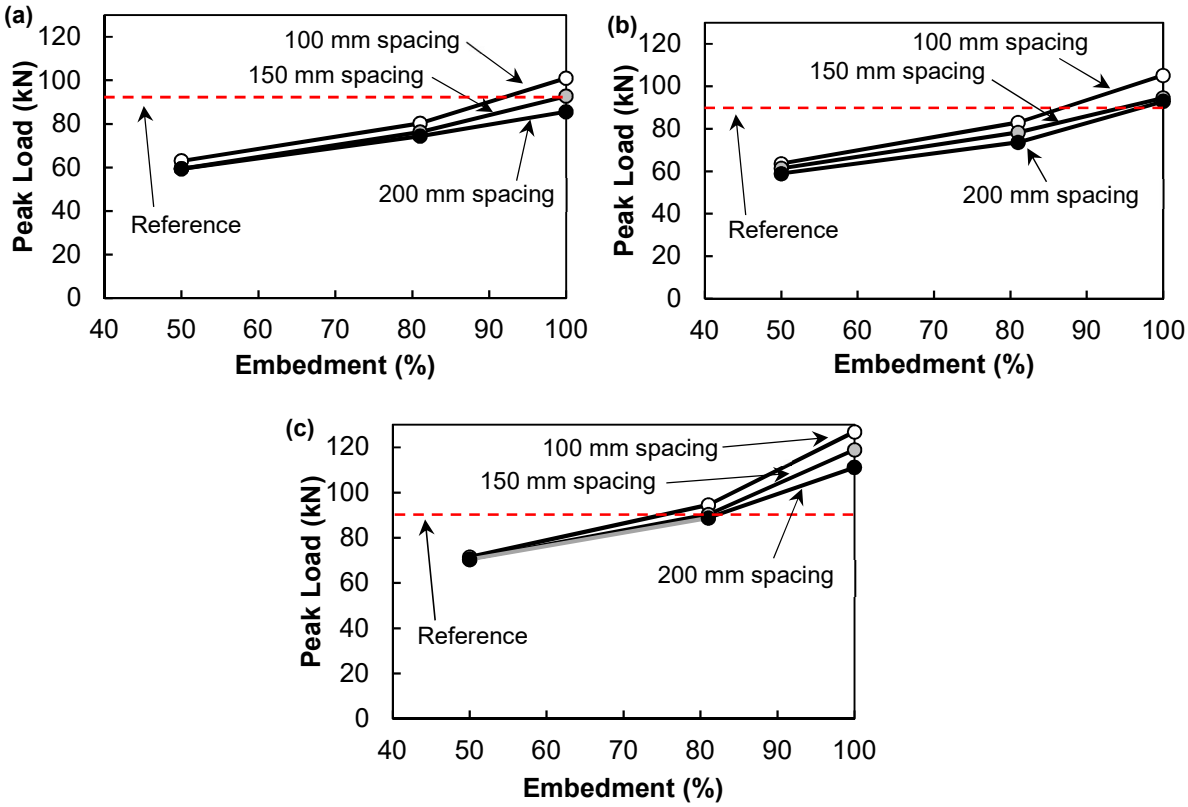

Figure 6: Effect of embedment ratio on barrier peak load for (a) 15 mm GFRP retrofit on 15M reinforced barrier (b) 20 mm GFRP retrofit on 15M reinforced barrier (c) 20 mm GFRP retrofit on 20M reinforced barrier.

4 CONCLUSIONS

Based on the findings obtained from VecTor2 set of models (number) on the behaviour of the steel-reinforced barriers, GFRP-reinforced barriers, and the barriers with the proposed repair techniques, and after studying the effect of changing some parameters on the design (diameter of GFRP reinforcing bars, and diameter of GFRP anchorage (single-headed bars), their spacing, and embedment ratio), the following conclusions can be drawn:

- Reinforcing bridge barriers with GFRP bars using 20M bars is a viable option since it achieved 92.1% of the ultimate load carrying capacity of its counterpart model reinforced with steel.
- Both repair techniques proved to be effective when the GFRP single-headed bars embedded across the full depth of the deck slab. They achieved an ultimate load carrying capacity higher than the one achieved by the undamaged barrier.
- In general, increasing the embedment ratio of the GFRP headed bars increases the strength of the repaired barriers.
- The effect of decreasing the spacing of GFRP single-headed bars on the strength of the repaired barriers is affected by the embedment ratios. For higher embedment ratios, the effect is maximized. In contrary, when the embedment ratio is low, the effect diminishes.
- The most efficient repair technique is using FRC and a single assembly of GFRP bars which achieved an ultimate load carrying capacity comparable to the one achieved by the as-built GFRP barrier while utilizing only one assembly of bars in the barrier wall. S

- The recommended design to replace the TL-4 Alberta steel-reinforced bridge barrier design is the 20M GFRP reinforced bridge barrier design instead of the equivalent reinforcement ratio design presented in the 15M GFRP reinforced bridge barrier.

5 FUTURE WORK AND RECOMMENDATIONS

- A parametric study on the effect of bar spacing and diameter of slab reinforcement, slab thickness, deck overhang, and concrete strength on the ultimate load carrying capacity of the bridge barrier will be conducted.
- Full scale static testing of the as-built prototypes of bridge barriers will be tested in the lab as well as the repaired ones to verify the validity of replacing steel bars with GFRP bars and to prove the efficiency of the proposed repair techniques for GFRP reinforced bridge barriers.
- Full scale static testing of bridge barriers of a width of three metres or more is strongly recommended to capture the two way behaviour and its contribution to the ultimate load carrying capacity of the bridge barriers.
- Full scale dynamic testing (crash testing) should be performed to prove the crashworthiness of the proposed GFRP reinforced bridge barriers design.

REFERENCES

AASHTO. 1989. *AASHTO Guide Specifications for Bridge Railings*, American Association of State Highway and Transportation Officials, Washington, D.C., USA

AASHTO. 2007. *AASHTO LRFD Bridge Design Specification. 4th Edition*, American Association of State Highway and Transportation Officials, Washington, D.C., USA.

Ahmed, E.A. and Benmokrane, B. 2011. Static Testing of Full-Scale Concrete Bridge Barriers Reinforced with GFRP Bars. *American Concrete Institute*, 275, 1-20.

Ahmed, E.A., Matta, F. and Benmokrane, B. 2013. Steel post-and-beam barrier with GFRP-reinforced concrete curb and bridge deck connection. *Journal of Bridge Engineering*, 18(11), 1189-1197.

Alberta Transportation. 2017. *TL-4 Single Slope Concrete Bridge Barrier Details*, *Standard Drawings and Typical Detail Drawings, Drawing No. S-1650-17*, Alberta Transportation, Edmonton, Alberta, Canada.

Azimi, H., Sennah, K., Tropynina, E., Goremykin, S., Lucic, S. and Lam, M. 2014. Anchorage Capacity of Concrete Bridge Barriers Reinforced with GFRP Bars with Headed Ends. *Journal of Bridge Engineering*, 9(19), 04014030.

Canadian Standard Association (CSA). 2014. *Canadian Highway Bridge Design Code*, CAN/CSA S6-14, Rexdale, Ontario, Canada, 894.

El-Salakawy, E., Mufti, A. and El-Ragaby, A. 2011. Laboratory investigations on the repair of GFRP-reinforced concrete bridge deck slabs. *Recent advances in maintenance and repair of concrete bridges*, American Concrete Institute, Farmington Hills, MI, USA, 277: 156–175.

El-Salakawy, E. and Islam, M. 2014. Repair of GFRP-Reinforced Concrete Bridge Barriers. *Journal of Bridge Engineering*, 19(6), 04014016.

TUF-BAR. 2019. *Product technical specifications*, TUF-BAR INC, Edmonton, Alberta, Canada.

Wong, P., Vecchio, F. and Trommels, H. 2013. *VECTOR2 & FORMWORKS USER'S MANUAL. Second Edition*, VecTor Analysis Group, Toronto, Ontario, Canada.